Available online at www.sciencedirect.com
SCIENCE DIRECT®
Journal of Molecular Structure 796 (2006) 23–27
Journal of MOLECULAR STRUCTURE
www.elsevier.com/locate/molstruc

Synthetic, structural and magnetic characterisation of a one-dimensional nickel chain constructed using *cis*,*trans*-1,3,5-triaminocyclohexane as a building block

Graham N. Newton [a], Geoffrey J.T. Cooper [a], De-Liang Long [a], Paul Kögerler [b], Leroy Cronin [a,*]

[a] *WestCHEM Department of Chemistry, The University of Glasgow, Glasgow G12 8QQ, UK*
[b] *Ames Laboratory and Department of Physics and Astronomy, Iowa State University, Ames, IA 50011, USA*

Received 1 February 2006; received in revised form 23 March 2006; accepted 30 March 2006
Available online 16 May 2006

Abstract

Complexation of Ni^{II} acetate with *cis*,*trans*-1,3,5-triaminocyclohexane (*trans*-tach) in the presence of acetic acid leads to the construction of an infinite one-dimensional nickel chain $\{[Ni_2(trans\text{-tachH})_2(OAc)_4(H_2O)_2](OAc)_2{\cdot}5H_2O\}_n$ (**1**). The crystal structure of **1** shows the chains to be connected via hydrogen bonded interactions between the protonated *trans*-amine group of the *trans*-tach and the non-coordinated oxygen atom of the acetate group bound to the second nickel centre on the parallel chain. Magnetic studies show ferromagnetic interactions between adjacent Ni^{II} centres.

Keywords: Self-assembly; One-dimensional chains; Hydrogen bonding; Rigid aliphatic ligands; Metal organic frameworks

1. Introduction

The self-assembly of coordination clusters is an area of interest to chemists due to the vast potential for creating clusters which exhibit interesting optical [1], catalytic [2] or magnetic properties [3]. Further research into this field may lead towards the rational design of molecular devices [4], and yield insight into the self-assembly processes which control their formation [5]. Specifically, the construction of infinite one-dimensional ferromagnetically coupled chains is of great interest due to their anisotropic magnetic properties [6]. In recent years much research has been focussed on the use of multidentate ligands as building blocks for extended supramolecular architectures due to their ability to coordinate to transition metals, as well as their potential to stabilise structures via non-coordinative interactions [5]. In this study the building block for chain formation is the sterically constrained aliphatic triamine ligand *cis*,*trans*-1,3,5-triaminocyclohexane (*trans*-tach) which has been shown to act both as a chelator and as a bridging ligand. Previous studies into the complexation behaviour of the ligand have yielded a range of interesting materials including polynuclear clusters [7,8], coordination networks [9] and one-dimensional chain complexes [10,11]. Herein we report the complexation of *trans*-tach with Ni^{II} in the presence of acetate anions leading to the formation of a *trans*-tach capped one-dimensional chain $\{[Ni_2(trans\text{-tachH})_2(OAc)_4(H_2O)_2](OAc)_2{\cdot}5H_2O\}_n$.

2. Experimental

Nickel acetate (97 mg, 0.390 mmol) was added in a 1:1 ligand to metal molar ratio, to a solution of *trans*-tach (50 mg, 0.388 mmol) in methanol (5 ml), which had previously been acidified to pH 7.5 via the dropwise addition of dilute acetic acid. This solution was stirred overnight

---

[*] Corresponding author. Tel.: +44 141 3306650.
E-mail address: L.Cronin@chem.gla.ac.uk (L. Cronin).

0022-2860/$ - see front matter © 2006 Elsevier B.V. All rights reserved.
doi:10.1016/j.molstruc.2006.03.087

until all solids were completely dissolved and was then set up for crystallisation by slow diffusion of diethyl ether into the mother liquor. After a period of approximately two weeks small, light blue, rhombus-shaped single crystals were formed in a yield of 38% (92 mg, 0.149 mmol, yield based on nickel). These were identified as **1** by single crystal X-ray structural analysis. Analysis of **1**: $\{[Ni_2(C_6H_{16}N_3)_2(OAc)_4(H_2O)_2](OAc)_2{\cdot}5H_2O\}_n$. Found (calcd): C, 34.08 (33.59); H, 7.50 (7.52); N, 9.22 (9.79); FTIR (KBr, cm^{-1}): 3424 (br s), 1559 (s), 1417 (s), 1125 (m), 1023 (m), 915 (m), 668 (m); UV–vis (MeOH, 293 K): ε (λ) 42 $mol^{-1}\,dm^3\,cm^{-1}$ (384 nm), 239 $mol^{-1}\,dm^3\,cm^{-1}$ (299 nm).

3. Results

The chain structure contains a dinuclear repeating unit in which two Ni^{II} centres are linked by bridging acetate anions with one metal centre being coordinated to the *cis*-amines of two ring-flipped *trans*-tach molecules in an *anti* arrangement, and the other being bound to two further acetate anions and two water molecules. These dinuclear subunits are linked to one another though bridging acetate anions and are stabilised by a further two acetate counter ions and five water molecules (Fig. 1).

Both Ni^{II} centres in the repeating unit of **1** have slightly distorted octahedral geometry with bond angles between 86.59(10)° and 93.41(10)° for the Ni^{II} bound to *trans*-tach and 84.11(8)° and 95.89(8)° for the other Ni^{II} centre. Thus, the geometry of the Ni^{II} bound only by acetate and water ligands is more distorted than that of the Ni^{II} coordinated by the two *trans*-tach ligands due to hydrogen bonded interactions (Table 1) between the acetate ligand and a *trans*-tach ligand on the neighbouring chain (Fig. 2). The *trans*-tach is bound with the two ligands arranged *anti* to one another with nickel–nitrogen bond lengths of 2.132(2) and 2.092(2) Å. The two Ni^{II} centres of each repeating unit are bridged by an acetate anion with nickel–oxygen bond lengths of 2.143(2) Å to the Ni^{II} bound to *trans*-tach and 2.071(2) Å to the other Ni^{II} centre. This longer bond to the *trans*-tach bound centre is caused by ligand bulk and the methyl group of the bridging acetate is forced away from the *trans*-tach molecule leading to a series of bends in the overall chain structure. This staggered arrangement is stabilised by hydrogen bonds of 3.044(3) Å

Table 1
Hydrogen bond lengths d(Å) and angles <(°)

D—H···A	d(D—H)	d(H···A)	d(D···A)	<(DHA)
N1—H1A···O6^{i}	0.92	2.29	3.044(3)	138.7
N2—H2C···O6	0.92	2.21	2.995(3)	142.5
N2—H2D···O8^{iv}	0.92	2.24	3.118(4)	158.4
N3—H3A···O9^{v}	0.91	1.97	2.864(4)	165.9
N3—H3B···O4^{vi}	0.91	1.86	2.758(4)	169.5
N3—H3C···O2^{ii}	0.91	1.86	2.764(3)	173.9
O7—H7A···O4^{ii}	0.83(2)	1.81(2)	2.634(3)	168(4)
O7—H7B···O2	0.82(2)	1.89(2)	2.699(3)	173(4)
O8—H8D···O1^{vii}	0.86(2)	1.93(3)	2.737(4)	157(6)
O8—H8E···O5^{viii}	0.86(2)	1.88(3)	2.687(3)	157(5)
O9—H9A···O10′^{iii}	0.86(2)	2.10(4)	2.91(2)	157(6)
O9—H9B···O1^{vii}	0.83(2)	1.92(2)	2.744(4)	174(7)

Symmetry transformations used to generate equivalent atoms: (i) $-x+1/2, -y+1/2, -z+1$; (ii) $-x+1, -y, -z+1$; (iii) $-x+1, y, -z+1/2$; (iv) $x, -y+1, -z+1/2$; (v) $-x+1/2, y-1/2, z+1/2$; (vi) $-x+1/2, -y+-1/2, -z++1$; (vii) $-x+1, -y+1, -z+1$; (viii) $-x+1/2, y+1/2, -x+1/2$.

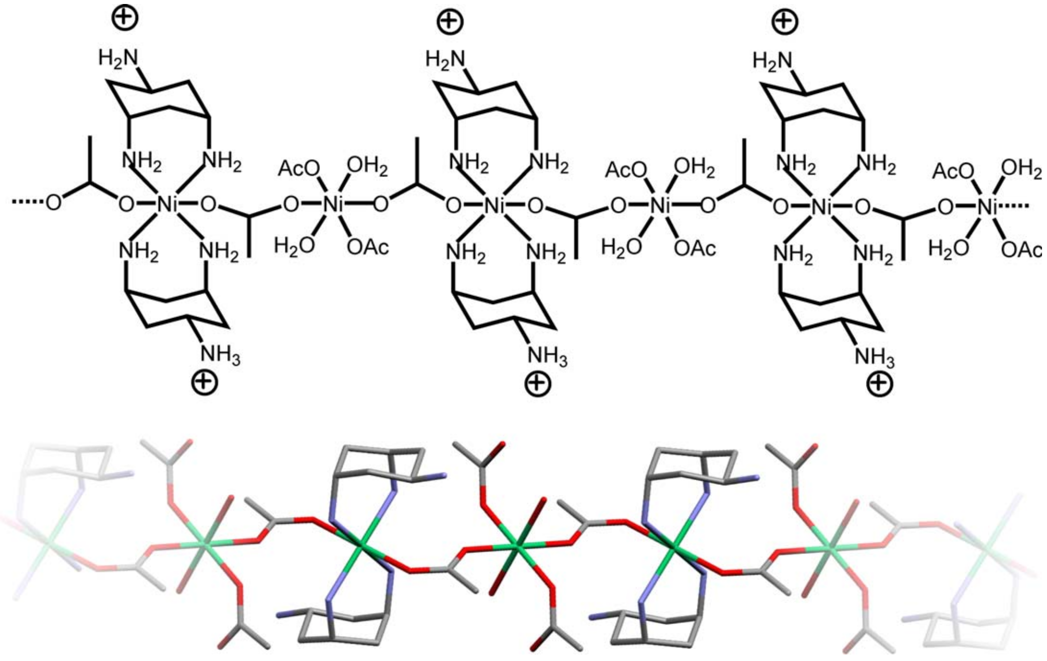

Fig. 1. Schematic representation (top) and crystallographically determined structure (bottom) of **1** with three repeat units shown. Nickel ions are shown in green, oxygen in red, nitrogen in blue and carbon in grey. (Solvent molecules and non-coordinated acetate anions are omitted for clarity.) (For interpretation of the references to color in this figure legend, the reader is referred to the web version of this paper.)

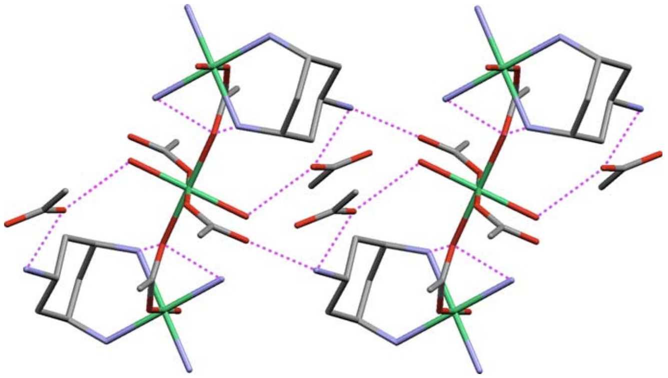

Fig. 2. Schematic representation of two parallel chains in the same layer illustrating the primary inter and intra-chain hydrogen bonded interactions (dashed lines) present in the structure. Nickel ions are shown in green, oxygen in red, nitrogen in blue and carbon in grey. (Solvent water molecules are omitted for clarity.) (For interpretation of the references to color in this figure legend, the reader is referred to the web version of this paper.)

and 2.995(3) Å between the *cis*-amino groups of the *trans*-tach ligands and the more distant oxygen atoms of the bridging acetate groups in the chain. The non-coordinating acetate anions provide further support to the chain by forming hydrogen bonded interactions with the protonated *trans*-amine of the ligand and the water ligand on the second Ni$^{\text{II}}$ centre, thus acting as bridging units. The coordination environment at the second Ni$^{\text{II}}$ centre is such that the two coordinated acetate ligands are arranged *anti* to one another so as to be perpendicular to the *trans*-tach ligands at the adjacent Ni$^{\text{II}}$.

The crystal-packing diagram of **1** (Fig. 3) shows a layered structure with each layer being comprised of sheets of parallel chain structures in the crystallographic ab-plane. The chains in each layer are bound to one another through hydrogen bonded interactions between the protonated *trans*-amine of the *trans*-tach ligands and the non-coordinated oxygen atoms of the acetate anions bound to the second Ni$^{\text{II}}$ centre with hydrogen bond distances of 2.758(4) Å. These layers are stacked throughout the crystal lattice and are sufficiently separated to prevent direct interaction between chains in different layers. The layers are however interconnected via hydrogen bonds between the protonated *trans*-amine group of *trans*-tach and a solvent water molecule. This in turn interacts with the uncoordinated acetate anion which bridges between *trans*-tach and water ligands through hydrogen bonded interactions with

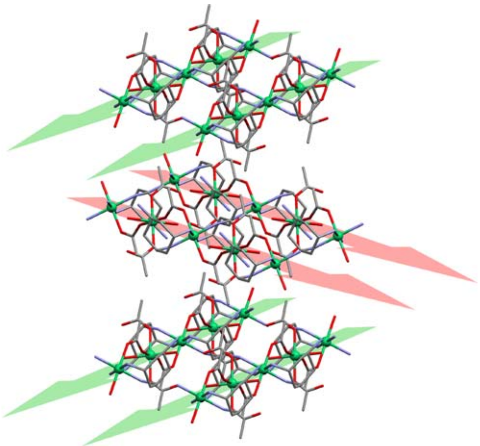

Fig. 3. Crystal-packing of **1** with arrows to show the direction of the chains. Red and green arrows are used to distinguish between the two layer types. Nickel ions are shown in green, oxygen in red, nitrogen in blue and carbon in grey. (All hydrogen atoms, solvent molecules and non-coordinated acetate anions are omitted for clarity.) (For interpretation of the references to color in this figure legend, the reader is referred to the web version of this paper.)

Table 2
Crystal data

Empirical formula	$C_{24}H_{64}N_6Ni_2O_{19}$
Crystal growth	Diffusion of diethyl ether, two weeks
Crystal description	Pale blue rhombic shapes
Crystal size	0.30 × 0.24 × 0.06 mm
Formula weight	858.23
Temperature	150(2) K
Wavelength	0.71073 Å
Crystal system	Monoclinic
Space group	$C2/c$
Unit cell dimensions	$a = 17.3058(6)$ Å $\alpha = 90°$
	$b = 11.1741(4)$ Å $\beta = 95.374(2)$ °
	$c = 20.8796(5)$ Å $\gamma = 90°$
Volume	4019.9(2) Å^3
Z	4
Calculated density	1.418 mg m^{-3}
Absorption coefficient	1.014 mm^{-1}
$F(000)$	1832
Theta range for data collection	2.34–25.99°
Reflections collected/unique	13,199/3933 [R(int) = 0.0382]
Completeness to theta	25.99 99.5%
Max. and min. transmission	0.9417 and 0.7507
Refinement method	Full-matrix least-squares on F^2
Data/restraints/parameters	3933/9/264
Goodness-of-fit on F^2	1.079
Final R indices [$I > 2\sigma(I)$]	$R1 = 0.0431$, $wR2 = 0.0915$
R indices (all data)	$R1 = 0.0769$, $wR2 = 0.1024$
Largest diff. peak and hole	0.70 and −0.53 e Å^{-3}

Table 3
Selected bond lengths (Å) and angles (°)

Ni1—N2	2.092(2)
Ni1—N1	2.132(2)
Ni1—O5	2.143(2)
Ni2—O7	2.061(2)
Ni2—O3	2.064(2)
Ni2—O6	2.071(2)
O7—Ni2—O3	87.38(9)
O7$^{\text{ii}}$—Ni2—O3	92.62(9)
O3$^{\text{ii}}$—Ni2—O6$^{\text{ii}}$	84.11(8)
N2—Ni1—N1	93.41(10)
N2—Ni1—N1$^{\text{i}}$	86.59(10)
N2—Ni1—O5$^{\text{i}}$	86.60(9)
N1—Ni1—O5$^{\text{i}}$	88.88(9)
N1—Ni1—O5	91.12(9)
O7—Ni2—O6$^{\text{ii}}$	93.67(9)
O3—Ni2—O6$^{\text{ii}}$	95.89(8)

Symmetry transformations as in Table 1.

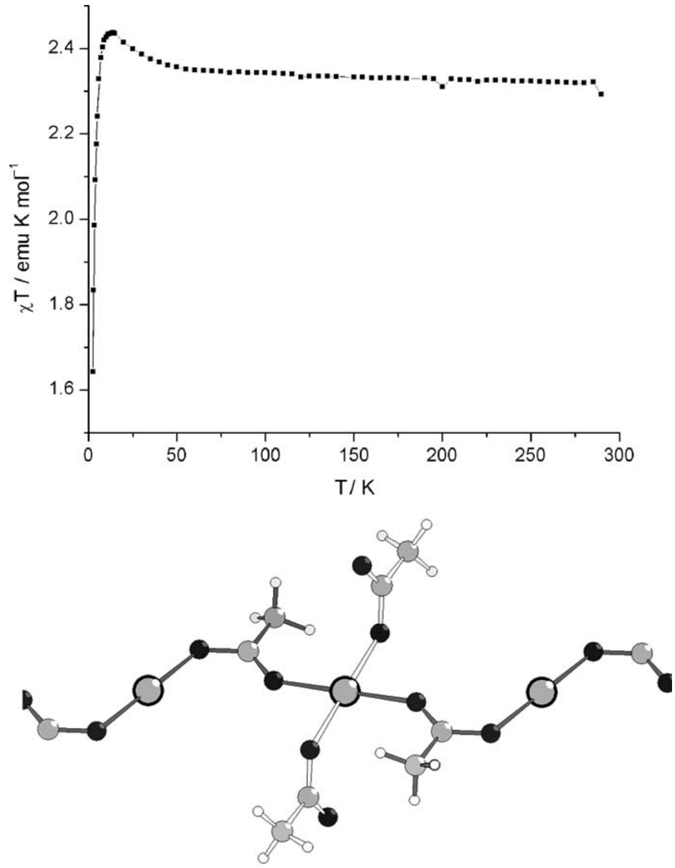

Fig. 4. (Top) temperature dependency of χT (corrected for diamagnetic contributions) at 0.1 T, showing the maximum at 14.0 K indicative of ferromagnetic coupling interactions. (Bottom) simplified representation of a section in the polymer structure of **1** showing three Ni^{II} centres (outlined spheres) with their bridging acetate positions (grey bonds, O: dark grey, C: grey, H: white) that mediate the ferromagnetic next-neighbour exchange and two acetate groups coordinated end-on to the central Ni^{II} centre (white bonds).

the neighbouring chain. Hydrogen bonds are also seen linking this anion, via another water molecule, to the acetate bridge adjacent to the *trans*-tach coordinated Ni^{II} in the chain. A further solvent water molecule is found between layers, disordered over four positions in a small range, riding on the twofold crystallographic axis and is connected to other water molecules through hydrogen bonded interactions (Tables 2 and 3).

The chains in adjacent layers are not parallel, leading to a repeating ABAB arrangement with chains in the "A" layer following the $(+a, +b)$ vector (defined by the crystallographic *a*- and *b*-axes) and those in the "B" layer following the $(+a, -b)$ vector. The chains in the two layers are therefore offset from one another by 33.3°, which is interesting in that this is also reminiscent of the angle seen at the sharper vertices of the crystals themselves, which are rhombus shaped.

The experimentally observed magnetism [12] of **1** (Fig. 4, top) indicates ferromagnetic coupling between next-neighbour $s = 1$ Ni^{II} sites as well as weaker antiferromagnetic (dipole–dipole) coupling between neighbouring chains. As the intra-chain super-exchange interactions only involve one type of bridging acetate configuration (Fig. 4, bottom) this system represents a ferromagnetic spin-1 Heisenberg chain. Based on simple model calculations on six-membered ring systems employing a Heisenberg Hamiltonian of the type $H = 2J\sum(S_iS_j)$ and an isotropic g factor of $g = 2.20$, we estimate the ferromagnetic nearest neighbour interaction to around $J \approx +0.8$ K (Fig. 5).

4. Conclusions

In conclusion, we have shown that the complexation of Ni^{II} with the ligand *trans*-tach leads to the formation of a one-dimensional chain, consisting of repeating Ni^{II} dimer units. This is stabilised by intra-chain hydrogen bonded interactions between the *cis*-amine of *trans*-tach and the distant oxygen of the neighbouring acetate group, and between the protonated *trans*-amine of *trans*-tach and the water ligand of the second Ni^{II} centre via a bridging acetate anion. Magnetic studies indicate that this system represents a ferromagnetic spin-1 Heisenberg chain.

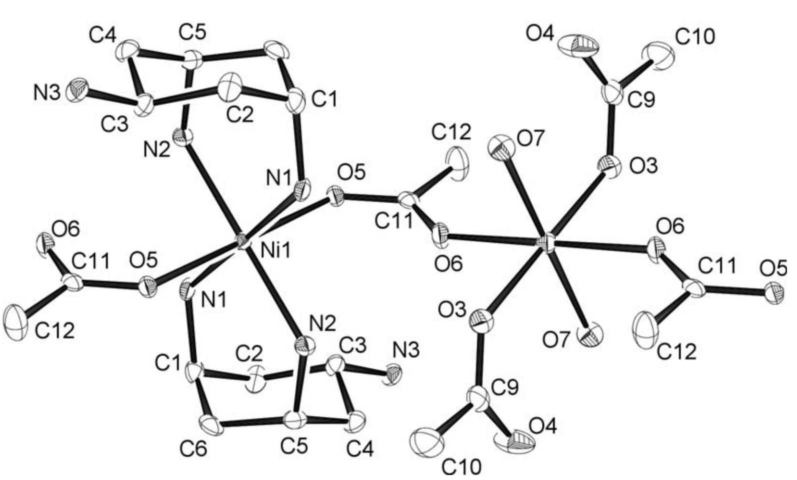

Fig. 5. Ortep-3 representation of $\{[Ni_2(trans\text{-tachH})_2(OAc)_4(H_2O)_2](OAc)_2\cdot 5H_2O\}_n$ (**1**): thermal ellipsoids at 50% probability. (All hydrogen atoms, solvent molecules and non-coordinated acetate anions are omitted for clarity.)

Acknowledgements

The authors are grateful to the EPSRC and the University of Glasgow for financial support.

Appendix A. Supplementary data

Supplementary data associated with this article can be found, in the online version, at doi:10.1016/j.molstruc.2006.03.087.

References

[1] H. Hou, Y. Wei, Y. Song, L. Mi, M. Tang, L. Li, Y. Fan, Angew. Chem. Int. Ed. Engl. 44 (2005) 6067–6074.

[2] N. Mizuno, M. Misono, Chem. Rev. 98 (1998) 199–217.

[3] R. Sessoli, H.-L. Tsai, A.R. Shake, S. Wang, J.B. Vincent, K. olting, D. Gatteschi, G. Christou, D.N. Hendriksen, J. Am. Chem. Soc. 115 (1993) 1804–1816.

[4] A.-M. Fuller, D.A. Leigh, P.J. Lusby, I.D.H. Oswald, S. Parsons, D.B. Walker, Angew. Chem. Int. Ed. Engl. 43 (2004) 3914–3918.

[5] J.-M. Lehn, Angew. Chem. Int. Ed. Engl. 29 (11) (1990) 1304–1319.

[6] P. Gambardella, A. Dallmeyer, K. Maiti, M.C. Malagoli, W. Eberhardt, K. Kern, C. Carbone, Nature 416 (2002) 301–304.

[7] G. Seeber, D.-L. Long, B.M. Karyuki, L. Cronin, Dalton Trans. (2003) 4498–4504.

[8] G. Seeber, P. Kögerler, B.M. Kariuki, L. Cronin, Chem. Commun. (2004) 1580.

[9] G. Seeber, A.L. Pickering, D.-L. Long, L. Cronin, Chem. Commun. (2003) 2002–2003.

[10] A.L. Pickering, D.-L. Long, L. Cronin, Inorg. Chem. 43 (2004) 4953–4961.

[11] J. Schnack, H. Nojiri, P. Kögerler, G.J.T. Cooper, L. Cronin, Phys. Rev. B. 70 (2004) 174420.

[12] Magnetic susceptibility measurements were performed for various fields (0.1–5.0 T) using a Quantum Design MPMSXL-5 magnetometer. Diamagnetic corrections ($\chi_{\mathrm{dia}}(\mathbf{1}) = -350 \times 10^{-6}$ emu mol^{-1}) were derived from tabulated values.